Geotextiles and Geomembranes 51 (2023) 93–103

Contents lists available at ScienceDirect

Geotextiles and Geomembranes

journal homepage: www.elsevier.com/locate/geotexmem

Regular Paper

Hydrodynamic assessment of bentonite granule size and granule swelling on hydraulic conductivity of geosynthetic clay liners

Juan Hou [a,b,*], Rui Sun [a], Craig H. Benson [c]

[a] School of Mechanics and Engineering Science, Shanghai Univ. Shanghai, 200444, PR China
[b] School of Engineering, Univ. of Virginia, Charlottesville, VA, 22904, USA
[c] Wisconsin Distinguished Professor Emeritus, Geological Engineering, University of Wisconsin-Madison, Madison, WI, 53706, USA

ARTICLE INFO

Keywords:
Geosynthetic clay liner
Hydraulic conductivity
Bentonite
Granules
Swelling

ABSTRACT

Flow in an idealized geosynthetic clay liner (GCL) containing bentonite comprised of equisized and equispaced square granules was simulated using a hydrodynamic model to quantitatively evaluate the premise that the hydraulic conductivity of GCLs diminishes as the bentonite granules hydrate and swell into adjacent intergranular pores, creating smaller and tortuous intergranular flow paths. Predictions with the model indicate that hydraulic conductivity decreases as granules swell and intergranular pores become smaller, and that greater granule swelling during hydration is required to achieve low hydraulic conductivity when the bentonite is comprised of larger granules, or the bentonite density is lower (lower bentonite mass per unit area). Predictions made with the model indicate that intergranular pores become extremely small (<1 μm) as the hydraulic conductivity approaches 10^{-11} m/s. These outcomes are consistent with experimental data showing that GCLs are more permeable when hydrated and permeated with solutions that suppress swelling of the bentonite granules, and that the hydraulic conductivity of GCLs with bentonite having smaller intergranular pores (e.g., GCLs with smaller bentonite granules, more broadly graded particles, or higher bentonite density) is less sensitive to solutions that suppress swelling.

1. Introduction

Geosynthetic clay liners (GCLs) are thin (7–10 mm) engineered barriers used to control the flow of liquids and the migration of contaminants in waste containment systems and other hydraulic structures. GCLs typically consist of a thin layer of granular or powdered sodium bentonite (typically 3.5–6.0 kg/m^2) sandwiched between two geotextiles that are bonded by needle punching or stitching (Fig. 1a). The sodium bentonite (NaB) in GCLs is in the form of particulate granules comprised of montmorillonite clusters with a small fraction of accessory minerals (e.g., quartz, calcite, etc.), as shown illustratively in Fig. 1b. Sodium cations are predominant in the exchange complex of the montmorillonite (Jo et al., 2001; Kolstad et al., 2004; Bradshaw and Benson 2014; Scalia et al., 2018; Rowe 2020).

The hydraulic conductivity of GCLs is controlled by the change in pore size and structure within a GCL that occurs in response to swelling of the montmorillonite during hydration, which is manifested at the macroscale as the swelling of the bentonite granules (Scalia et al. 2011, 2018; Chen et al., 2018, Gustitus et al., 2021; Norris et al. 2022a, 2022b). As the bentonite granules swell, the size of the intergranular pores diminishes and the tortuosity of the intergranular pore space increases, as illustrated by the photographs in Fig. 2 for bentonite from a GCL containing sand-size granular bentonite.

Prior to hydration, relatively large intergranular pores exist between the bentonite granules in the GCL (Fig. 2a) that are comparable to those in a sand with similar size particles. As the bentonite hydrates, the bentonite granules swell and expand into the adjacent intergranular pore space. When hydrated with liquid that promotes swelling such as deionized water (DW), the bentonite granules swell appreciably, closing intergranular pores as illustrated in Fig. 2b and resulting in low hydraulic conductivity (Petrov and Rowe 1997; Jo et al., 2001; Kolstad et al., 2004; Scalia et al., 2018). For hydrating solutions that suppress swell, some intergranular pores remain open and the hydraulic conductivity is higher, as illustrated in Fig. 2c for granular bentonite hydrated with a 250 mM $CaCl_2$ solution. When the hydrating solution suppresses granule swelling extensively, as illustrated in Fig. 2d for granular bentonite hydrated with a 500 mM $CaCl_2$ solution, the intergranular pores remain open, and the hydraulic conductivity is very high.

* Corresponding author. School of Engineering, Univ. of Virginia, Charlottesville, VA, 22904, USA.
E-mail addresses: juanhou@staff.shu.edu.cn (J. Hou), sunrui6@shu.edu.cn (R. Sun), chbenson@wisc.edu (C.H. Benson).

https://doi.org/10.1016/j.geotexmem.2023.05.002
Received 6 July 2022; Received in revised form 28 April 2023; Accepted 16 May 2023
Available online 1 June 2023

Flow paths along needlepunching fiber bundles or stitching are influenced in a similar manner by swelling of bentonite (Bareither et al., 2017; Norris et al. 2022a, 2022b). When granule swelling is highly suppressed, the hydraulic conductivity can approach hydraulic conductivities characteristic of materials having similar particle size as the unhydrated bentonite, i.e., non-plastic silt for powdered bentonite ($\approx 10^{-8}$ m/s) or sand for granular bentonite ($\approx 10^{-6}$ m/s). The magnitude of granule swelling and the reduction in hydraulic conductivity depend on the ionic strength and relative abundance of monovalent and polyvalent cations in the hydrating solution (e.g., Jo et al., 2001; Kolstad et al., 2004; Hou et al., 2022).

A two-dimensional hydrodynamic model was used in this study to examine quantitatively how swelling of granules and closure of intergranular pores affects the hydraulic conductivity of an idealized GCL, as described conceptually and observed experimentally by others (Scalia et al. 2011, 2018; Chen et al., 2018, Rowe 2020, Gustitus et al., 2021; Norris et al. 2022a, 2022b). The model was implemented using COMSOL Multiphysics 5.4, a flexible software package for solving partial differential equations using the finite-element method (COMSOL 2021). Simulations were conducted to evaluate how intergranular flow and hydraulic conductivity are affected by granule shape, granule size, bentonite dry density (granules per unit volume), and granule swelling. Hydraulic conductivity of the idealized GCL was computed from the velocity of the pore water at the effluent boundary of the domain. The outcomes from the model apply to conditions in response to hydration and swelling of the bentonite granules during permeation. Impacts associated with subsequent changes in the chemistry of the permeant solution or the physical environment imposed on the GCL after hydration and swelling are not addressed, and would require additional features in the model.

2. Hydraulic model

2.1. Conceptual model

The conceptual model consists of a control volume comprised of bentonite granules and intergranular pores between the granules, shown illustratively in Fig. 3. Actual granules are more complex, being comprised of a collection of montmorillonite clusters with complex lamellar structure as well as accessory minerals (e.g., as shown illustratively in Fig. 1b). In this study, the objective was to evaluate how swelling of bentonite granules during hydration in response to a known permeant solution affects the flow in macroscale intergranular pores and the hydraulic conductivity of a GCL. In the context of this objective, incorporating microscale features within granules or clusters was not necessary. Alterations in the permeant chemistry or physical condition imposed on the GCL subsequent to hydration and swelling may alter both intergranular pores and microscale features, and also affect hydraulic conductivity. These effects were not within the objective of this study and would need to be addressed with additional features in the model.

Water within the bentonite in the GCL was assumed to be reside in two distinct phases: a highly mobile phase in the intergranular pores between the bentonite granules (Fig. 3) and a less mobile phase within the granules, where water interacts with mineral surfaces or resides in the fine pores within and between mineral phases (Fig. 1b). The two water phases were assumed hydraulically independent, and water flow in the intragranular pores was assumed to be negligible relative to flow in the intergranular pores. In an actual GCL, these two phases will interact, with the role of the less mobile phase within granules increasing as the intergranular pores close in response to swelling of the bentonite granules.

When granule swelling is suppressed during hydration and GCLs are more permeable, intergranular flow is hypothesized to be predominant, with flow through the fine intragranular pores neglible (Fig. 3b) (Scalia and Benson, 2010; Tian et al., 2019; Gustitus et al., 2021, Scalia et al., 2018; Norris et al. 2022a, 2022b). In effect, the granules in a more permeable GCL are assumed to function like impermeable inclusions with flow occurring almost exclusively in the adjacent intergranular pores space (Fig. 3b). Water flow in the intergranular pores is controlled by the size, shape, connectedness, and tortuosity of the intergranular pore space, which are influenced by the size, shape, and arrangement of the granules comprising the bentonite in the GCL. The hydrodynamic model used in this study simulated the conditions illustrated schematially in Fig. 3b and c and shown photographically in Fig. 2c and d, approaching but not including the limiting state shown schematially in Fig. 3d and illustrated by the photograph in Fig. 2b. Sealing of reinforcing fibers was not modeled, and was assumed to occur concurrent with closure of intergranular pores.

Porosity of the bentonite was assumed to consist of an intergranular porosity (n_i) comprised of the volume of intergranular pore space of mobile water active in flow (V_p) and a less mobile porosity (n_l)

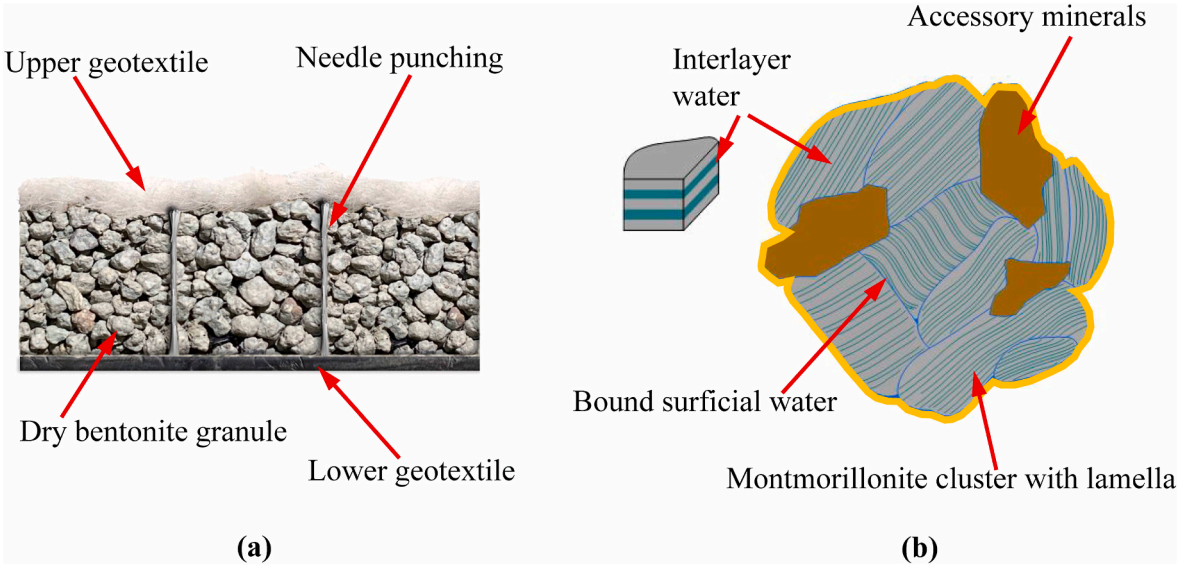

Fig. 1. GCL with granular bentonite prior to hydration and swelling (a) and conceptual diagram of bentonite granule comprised of montmorillonite clusters and accessory minerals with layer associated with the external and interlayer surfaces of the clusters (b). Bentonite granule comprised of several montmorillonite clusters intermingled with secondary minerals. Conceptual diagram in (b) adapted from Bradbury and Baeyens (2002).

comprised of pores containing less mobile water (e.g., pores within granules as well as dead end and occluded intergranular pores). The sum of these porosities is the total porosity ($n = n_i + n_l$), defined as the total volume of pores per unit total volume of bentonite (V_b). The volume of bentonite (V_b) equals the sum of the volume of granules (V_g) and the volume of the intergranular pores (V_p), which is assumed fixed, with expansion constrained by the needle-punching fibers binding the upper and lower geotextiles in the GCL. This is an approximation, as the total volume of bentonite in a GCL increases during hydration until tension in the needle-punching fibers is sufficient to balance the swelling pressure exerted by the bentonite. As granule swelling increases, V_g increases and V_p decreases, with $V_p \rightarrow 0$ and $V_b \rightarrow V_g$ in the limiting state.

2.2. Hydraulic model and fluid dynamics

A two-dimensional hydraulic model was created using the flexible partial differential equation solver COMSOL Multiphysics 5.4 (COMSOL, 2021) using a simplified geometry that approximates the conceptual model illustrated in Fig. 3. A square domain was assumed that is comprised of granules uniform in shape and size that are vertically stacked and uniformly distributed in the domain. Granules were assumed to have an initial (prior to hydration) predominant granule dimension (e.g., width or diameter), w_0. The granules were aligned along the rectangular grid as shown in Fig. 4 (i.e., vertical stacks), with flow occurring through a structured set of intergranular pores between the granules having a pore throat width. The granules were assumed to

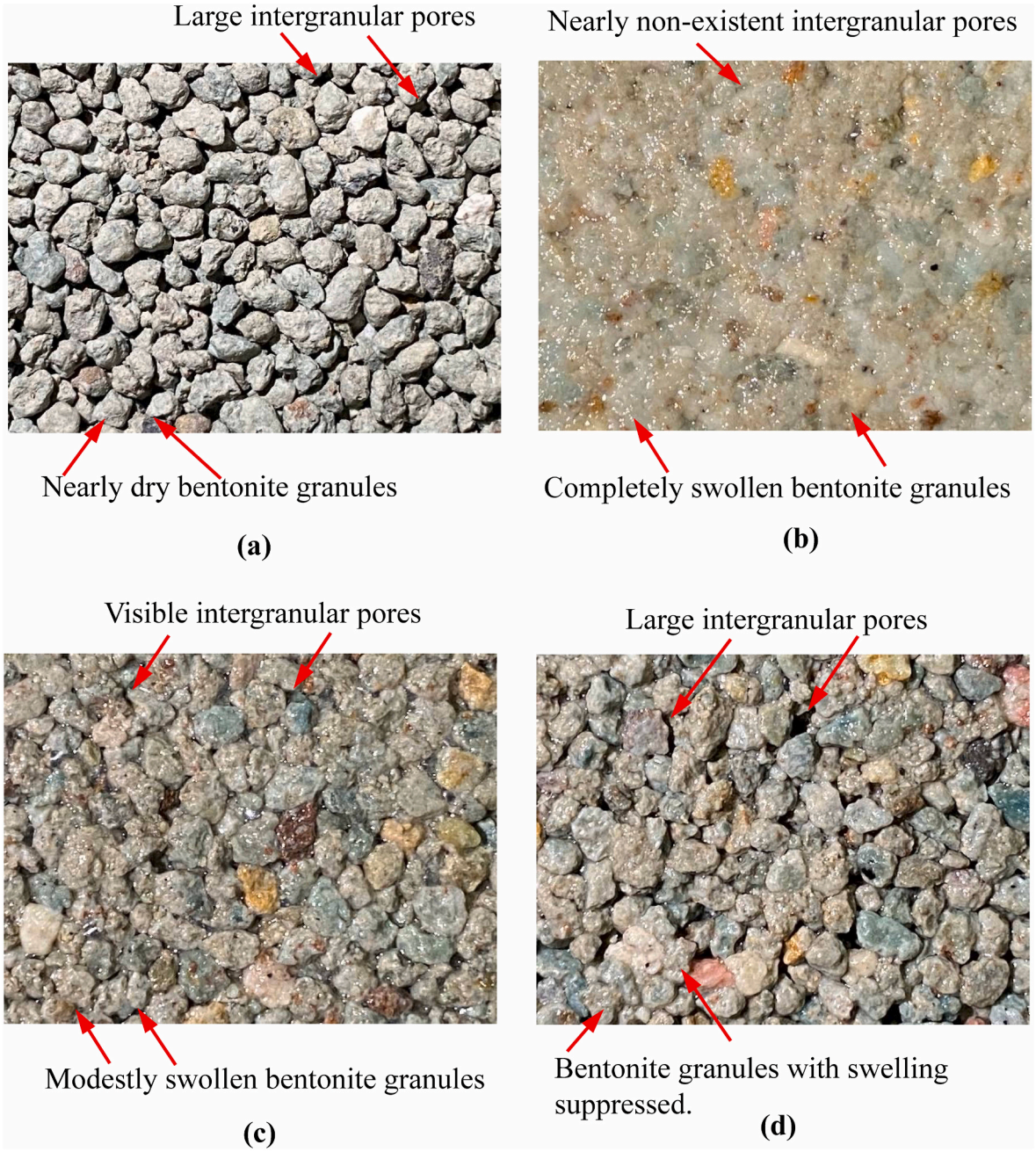

Fig. 2. Bentonite granules in different states of hydration and swelling: (a) air-dry bentonite granules prior to hydration and swelling, and (b) swollen bentonite granules hydrated in DIW for 48 h with nearly non-existent intergranular pores, (c) bentonite granules hydrated in 250 mM $CaCl_2$ solution for 48 h showing suppressed swelling and visible intergranular pores, and (d) bentonite granules hydrated in 500 mM $CaCl_2$ solution for 48 h showing completely suppressed swelling and large intergranular pores.

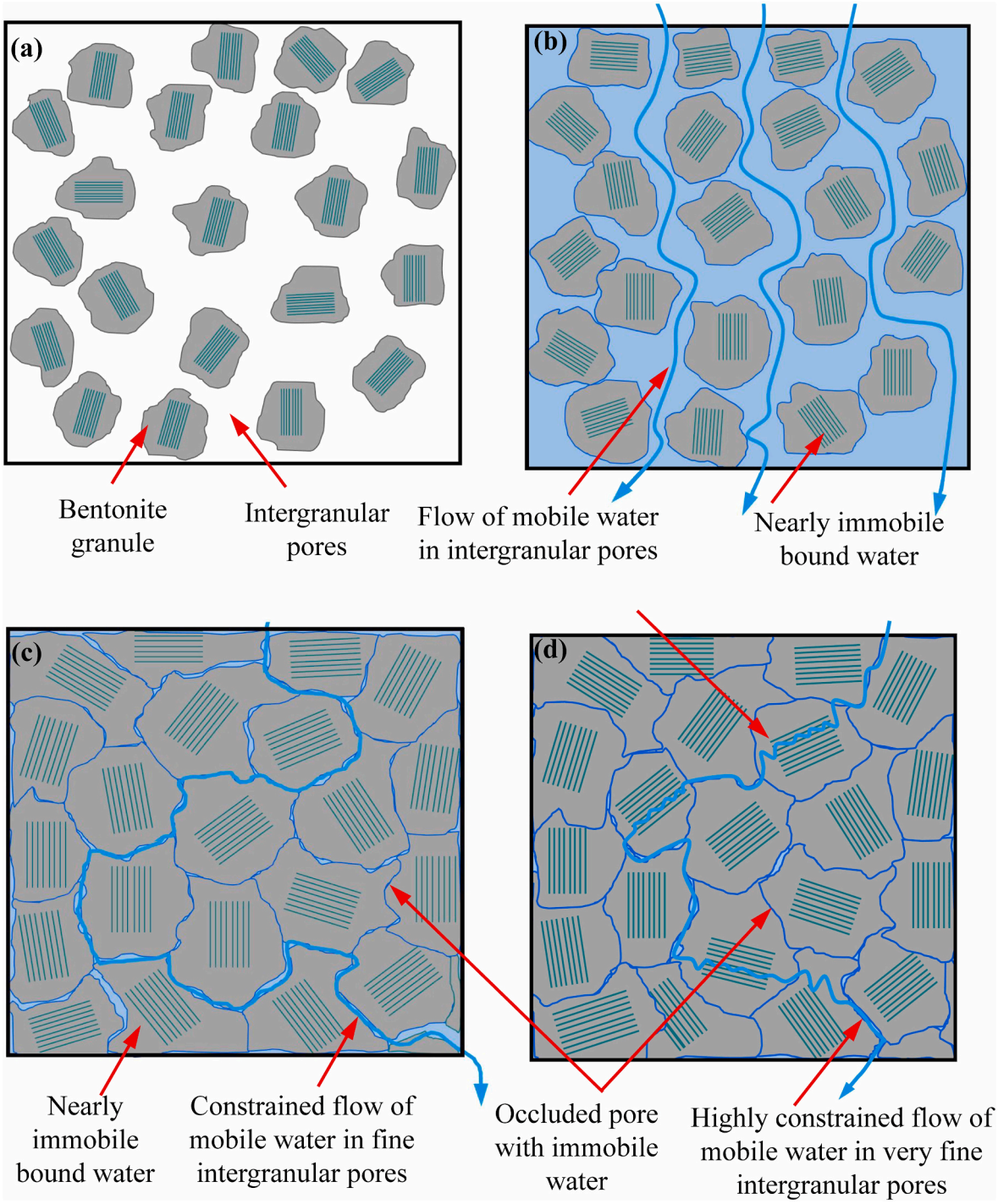

Fig. 3. Conceptual model of bentonite granules, intergranular pores, and flow paths for different states of hydration and swelling: (a) unhydrated granules with large intergranular pores, (b) hydrated granules with modest swelling and relatively unconstrained flow through large intergranular pores, (c) hydrated granules with high granule swelling and constrained flow in fine and tortuous intergranular pores, and (d) hydrated granules with very high swelling and nearly closed intergranular pores, with flow in fine and very tortuous intergranular and intragranular pores.

be impermeable, with flow occurring only in the intergranular pore space. The pore throat width was assumed constant throughout the domain.

The Reynold's number (R_e) for the idealized bentonite was computed to assess the type of flow occurring in the intergranular pore space:

$$R_e = \frac{\rho v w_p}{\eta} \quad (1)$$

where ρ is the density of the intergranular pore water (1 kg/L), η is the dynamic viscosity of the intergranular pore water (0.001 Pa s), v is the seepage velocity, and w_p is the largest pore width in the domain. For the assumed geometry, the largest possible R_e for a given granule size corresponds to the case with no swelling and the highest possible seepage velocity. This seepage velocity can be computed for a GCL hydraulic conductivity of 10^{-7} m/s (very permeable) and total porosity (n) of 0.4 (Chen et al., 2018). For typical geometries used in the analysis (described subsequently), the largest pore width (w_p) is at most 0.264 mm, corresponding to a dry mass unit area (4800 kg/m^2) and large

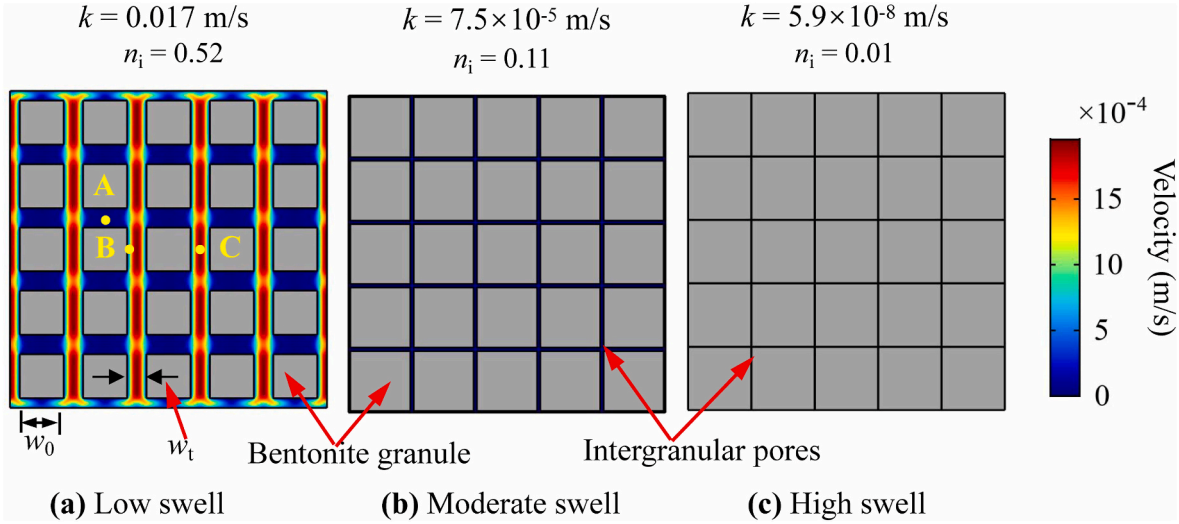

Fig. 4. Idealized model of flow through intergranular pores in GCL with square bentonite granules and various degrees of swelling: (a) low granule swelling and larger intergranular pores, (b) moderate granule swelling and small intergranular pores, and (c) higher granule swelling and fine intergranular pores. Color in pore space corresponds to fluid velocity in legend. Predominant granule dimension = w_o and pore throat width = w_t.

granules. This condition yields a seepage velocity of 1.58×10^{-8} m/s and $R_e = 1.56 \times 10^{-6}$.

For $R_e \ll 1$, creeping flow is predominant and the Navier-Stokes equations are (Panton, 2013):

$$\rho \nabla \cdot \boldsymbol{v} = 0 \tag{2a}$$

$$0 = -\nabla p + \nabla \cdot \eta\left(\nabla \boldsymbol{v} + (\nabla \boldsymbol{v})^{\mathrm{T}}\right) \tag{2b}$$

where ρ is the density of the intergranular pore water (kg/L), $\boldsymbol{v}$ is the velocity vector (m/s), p is the fluid pressure, and superscript "T" represents transpose. For creeping flow, viscous effects are predominant and gravity effects are negligible.

Eqs. (2a) and (2b) were solved as stationary in time using the finite element method (FEM) implemented in the fluid dynamics software COMSOL for the geometry shown in Fig. 4. Flow was assumed to occur upward with a constant head on the lower horizontal surface (inlet pressure = 1 Pa) and a constant head on the upper horizontal surface (outlet pressure = 0 Pa). The left and right vertical surfaces were no flow boundaries. A typical finite-element mesh used in the simulations is shown in Fig. 5. A physics-controlled triangular extremely fine mesh was employed for high precision and accuracy, while reducing memory requirements and execution time. The maximum number of iterations was set at 100 and the velocity tolerance less than 0.001 m/s. The solution consists of the steady-state distribution of fluid pressure and velocity within the domain. The velocity distribution across the upper surface (outflow boundary) was integrated and then normalized by the gross area of the outflow boundary to obtain the Darcy flux, q. The hydraulic conductivity of the domain (K) was then computed as the ratio, $K = q/i$, where i is the hydraulic gradient. The solution was verified for a limiting case with two stacks of granules, approximating flow between parallel plates as described by the Hagen-Poiseuille (Panton, 2013). Excellent agreement was obtained, as illustrated in the Appendix.

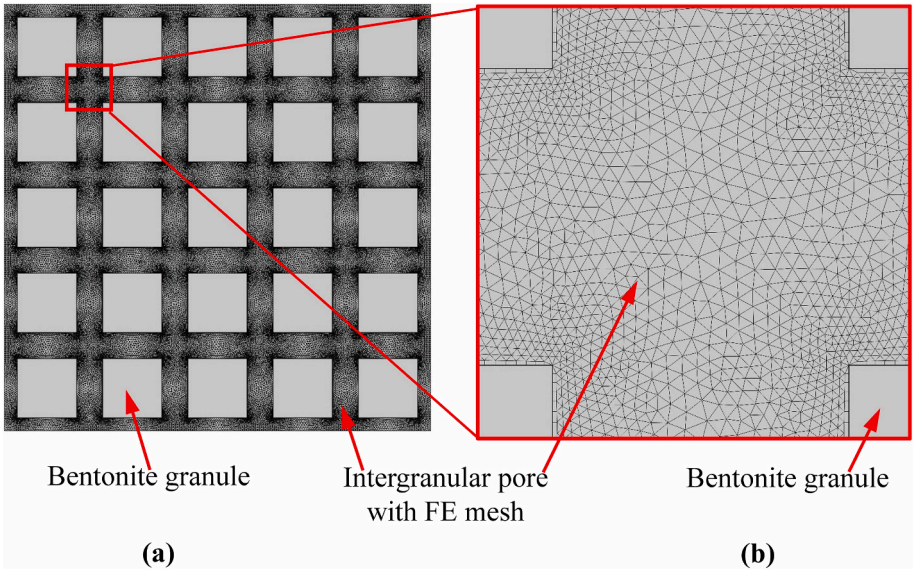

Fig. 5. Domain comprised of impermeable square bentonite granules (gray) with finite element (FE) mesh in intergranular pores (a) and blow up of finite element mesh at junction of intergranular pores adjacent to four neighboring bentonite granules.

2.3. Granule and domain characteristics

The granule shape, number of granules, and the domain dimensions were evaluated by conducting sensitivity analyses that varied the granule shape (circle, square, or diamond, Fig. 6), number of granules (Fig. 7), and the intergranular porosity (Fig. 7). The particle shapes considered in Fig. 6 are an approximation of actual bentonite granules in GCLs, which have an irregular angular surface (Fig. 2a). All simulations consisted of vertical stacks of granules. The domain height was set at 7 mm to represent a typical GCL thickness (Bradshaw et al., 2014) and the granule dimension was varied between 0.002 and 1.5 mm to represent typical granule sizes in GCLs ranging from powdered to granular bentonite (Kolstad et al., 2004). The initial (pre-swelling) intergranular porosity (n_0) was varied between 0.3 and 0.6.

Essentially the same hydraulic conductivities were obtained with the square (Fig. 6a) and circular granules (Fig. 6b), whereas lower hydraulic conductivities were obtained with the diamond granules (Fig. 6c). For example, for $n_0 = 0.6$ (no granule swelling), a granule dimension of 0.1 mm, and 25 granules in the domain (0.8 mm × 0.8 mm), the following hydraulic conductivities were obtained: $1.12\text{x}10^{-3}$ m/s (square), $1.15\text{x}10^{-3}$ cm/s (circle), and $2.92\text{x}10^{-4}$ m/s (diamond). Lower hydraulic conductivity was obtained with the diamond-shaped granules due to smaller pore throats, all other factors being equal (Fig. 6).

The effect of intergranular porosity (n_i) and the number of granules is shown in Fig. 7. Intergranular porosity was varied from 0.01 to 0.998 and the number of granules was varied between 25 and 225, bracketing the number of granules used in the analyses. The pore width and porosity were maintained consistent while increasing the number of granules by increasing the domain size accordingly. Essentially the same outcomes were obtained for 25 and 225 granules, indicating that domains with at least 25 granules are sufficient to represent the flow regime used to compute hydraulic conductivity of the idealized bentonite. The hydraulic conductivity also decreases substantially as the intergranular porosity decreases because of the decrease in size of the intergranular pores (0.26 mm–0.004 mm) as the granules swell, indicating that the model yields the expected behavior as the size of the intergranular pores diminishes.

For geometric simplicity, all simulations to assess the impact of granule swelling on pore size and hydraulic conductivity were conducted with square impermeable granules arranged on a rectangular grid like that shown in Fig. 4, with flow occurring only between the granules and the boundary conditions described in the discussion of Fig. 6. This geometric arrangement is a simplification of the actual pore space, but was considered sufficient to quantitatively evaluate the underlying conceptual model that reductions in the size of intergranular pores due to swelling of bentonite granules results in lower hydraulic conductivity. The granule size was varied from 0.002 mm to 1.5 mm, representing powered bentonites (<0.08 mm) and granular bentonites (>0.08 mm), and the initial intergranular porosity was varied from 0.3 to 0.6 to represent different bentonite densities (granules per volume). The permeant solution in the pores was assumed to have the hydrodynamic properties of water, as described previously.

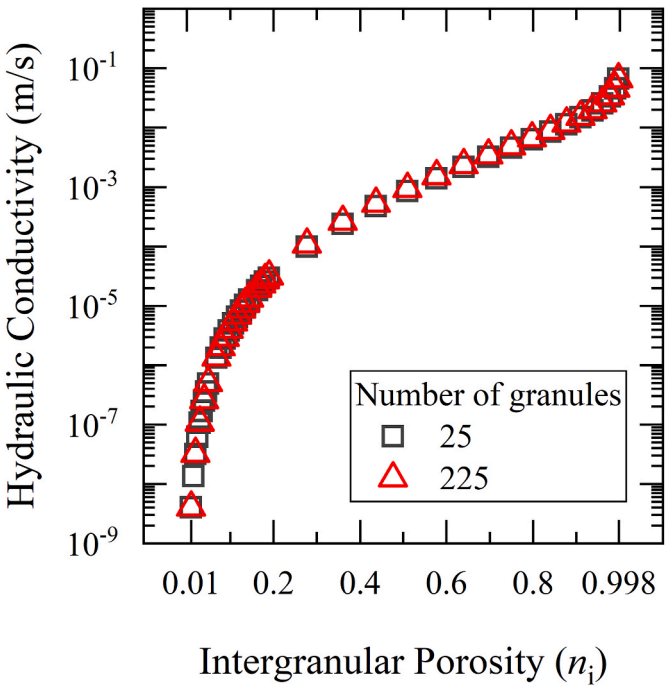

Fig. 7. Hydraulic conductivity vs. intergranular porosity for 25 and 225 granules.

3. Results and discussion

3.1. Swelling, flow velocities, and hydraulic conductivity

The effect of granule swelling during hydration on n_i, intergranular pore water velocities, and hydraulic conductivity is illustrated in Fig. 4. The intergranular pore velocities decrease dramatically as the granules swell into the intergranular pores and the intergranular porosity diminishes. The velocities shown in Fig. 4 also illustrate how flow velocity within the intergranular pore space varies spatially, and how the pore water velocity (analagous to seepage velocity) differs from the Darcy velocity. For example, in Fig. 4a, the pore water velocity at Point A in a horizontal pore (1.71×10^{-5} m/s) is very low, the velocity at Point B near a pore wall (1.08×10^{-4} m/s) is higher, and the pore water velocity in the center of the pore at Point C is highest (1.94×10^{-3} m/s). The average velocity across the discharge face, also known as the Darcy velocity (3.97×10^{-4} m/s), is lower than the average pore water

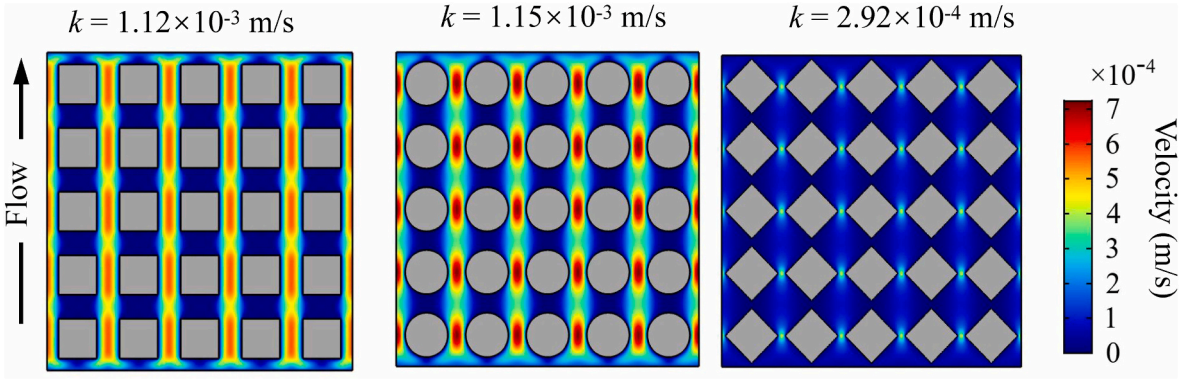

Fig. 6. Model domain with granules having different shape and similar primary dimension (0.1 mm): (a) square, (b) circular, and (c) diamond.

velocity (1.34×10^{-3} m/s) and the peak pore water velocity (1.95×10^{-3} m/s).

3.2. Granule size and intergranular porosity

Hydraulic conductivity predicted by the model is shown in Fig. 8 as a function of intergranular porosity (n_i) for an initial predominant granule dimension (w_0) ranging from 0.005 to 1.5 mm. The variation in n_i represents the reduction in size of the intergranular pores as granules swell and fill the adjacent intergranular pore space. For a given w_0, the hydraulic conductivity decreases as n_i diminishes (swelling increases) because the intergranular pores become smaller, constraining flow (e.g., as shown in Fig. 4). Similarly, for the same n_i, the hydraulic conductivity is lower for smaller w_0 because smaller intergranular pores coincide with smaller granules. For example, when $n_0 = 0.3$, the hydraulic conductivity for granules with $w_0 = 0.005$ mm is about five orders of magnitude lower than the hydraulic conductivity for granules with $w_0 = 1.0$ mm. For $n_0 = 0.3$, the pore width (w_t) is 0.001 mm for granules with $w_0 = 0.005$ mm, and $w_t = 0.2$ mm for granules with $w_0 = 1.0$ mm. That is, without substantive granule swelling during hydration, a powdered bentonite will have lower hydraulic conductivity than a granular bentonite all other factors being equal.

The hydraulic conductivities in Fig. 8 vary over a very broad range that spans from conditions characteristic of coarse sand (high n_i and large w_0) to conditions characteristic of clay (lower n_i and smaller w_0), depending on the intergranular porosity and the predominant granule size. The rate of change in hydraulic conductivity increases dramatically as n_i approaches zero (Fig. 8). For w_0 comparable to typical granule sizes in granular bentonites in GCLs ($w_0 = 0.3$–0.9 mm), the hydraulic conductivities range from approximately 0.01 m/s ($n_i = 0.6$, no swellling) to near 10^{-11} m/s ($n_i = 0.01$, high swelling). For w_0 comparable to typical granules in powdered bentonites in GCLs ($w_0 = 0.005$–0.05 mm), the hydraulic conductivities range from approximately 10^{-4} m/s ($n_i = 0.6$, no swellling) to less than 10^{-11} m/s ($n_i = 0.01$, high swelling). This range of hydraulic conductivities brackets the range of hydraulic conductivities observed for GCLs with granular and powdered bentonites for different states of hydration and swelling (Kolstad et al., 2004; Scalia et al., 2018).

The role of granule swelling during hydration in achieving low hydraulic conductivity depends on the granule density and granule size, as shown in Fig. 9 in terms of the granule swelling ratio (S_r), defined as the increase in cross-sectional area of the granule relative to the initial cross-sectional area prior to granule swelling:

$$S_r = \frac{\left(w_s^2 - w_0^2\right)}{w_0^2} \tag{3}$$

where w_s is the predominant granule dimension after swelling. All granules were assumed to swell uniformly, and all granules were assumed to swell the same amount. Simulations were conducted that represented high density bentonites (initial intergranular porosity, $n_0 = 0.3$), intermediate density bentonites ($n_0 = 0.4$), and low density bentontes ($n_0 = 0.6$).

The swelling ratio required to achieve a particular hydraulic conductivity is much greater for high n_0, representing a GCL with a low bentonite density and larger intergranular pores, than for simulations with low n_0, representing a GCL with a high bentonite density, all other factors being equal (Fig. 9). Similarly, for a given n_0, much greater swell ratio is required to achieve a given hydraulic conductivity for simulations with large granules (high w_0) relative to those with smaller granules (small w_0). The importance of granule swell ratio follows directly from the initial size of the intergranular pores, which are much larger for simulations representing low density bentonite (high n_0) with large particles (high w_0) relative to simulations representing high density bentonite (low n_0) with small particles (low w_0).

The relative roles of w_0, n_0, and n_i are illustrated in Fig. 10a ($w_0 = 0.0$–1.55 mm) and Fig. 10b (close up for $w_0 = 0.0$–0.08 mm). The predictions in Fig. 10a represent all granule sizes, whereas Fig. 10b represents fine granular and powdered bentonites. The hydraulic conductivity decreases as w_0 or n_i decreases (i.e., lower hydraulic conductivity for smaller granules and lower intergranular porosity), and is relatively insensitive to n_0 for a given n_i. However, achieiving sufficiently low n_i to achieve specific hydraulic conductivity for a given w_0 requires greater granule swelling as n_0 increases. Thus, GCLs comprised of bentonite with larger granules (larger w_0) or lower bentonite density (larger n_i) must have greater granule swelling during hydration to

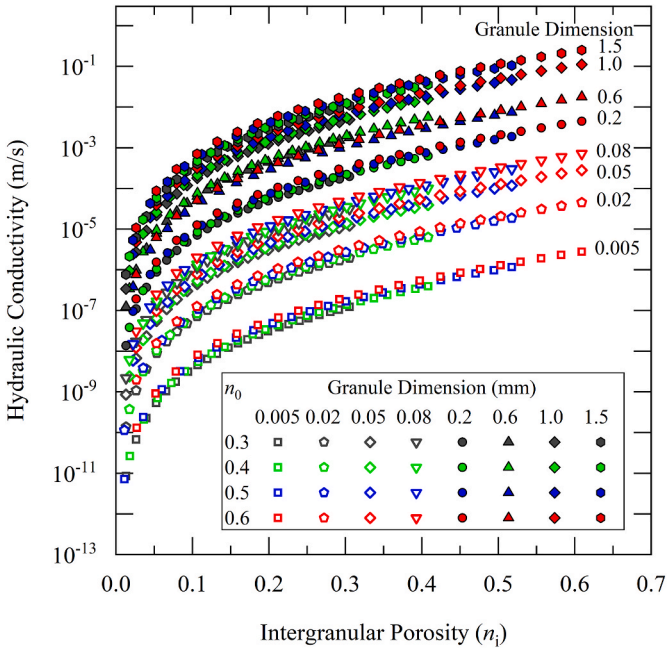

Fig. 8. Hydraulic conductivity of domain as a function of intergranular porosity (n_i) for different predominant granule dimensions ($w_0 = 0.005$–1.5 mm) and initial intergranular porosity ($n_0 = 0.3$–0.6).

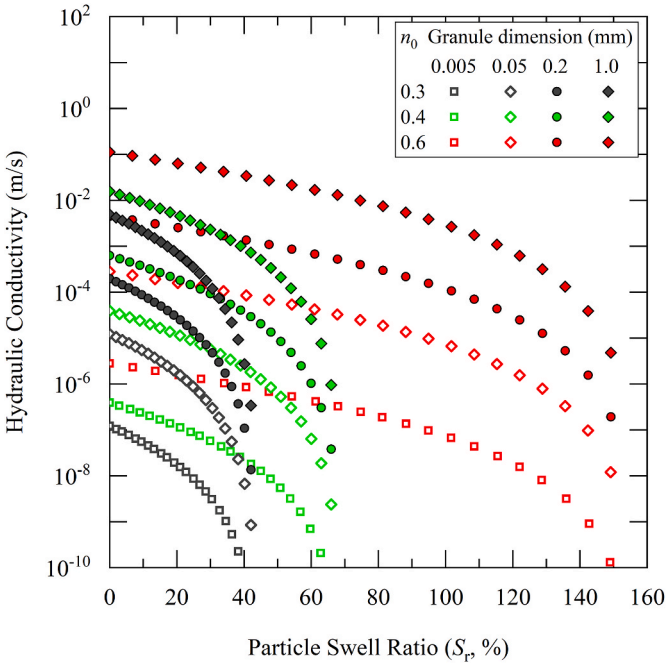

Fig. 9. Hydraulic conductivity of domain as a function of swell ratio of granules (S_r) for different predominant granule dimensions ($w_0 = 0.005$–1.000 mm) and initial intergranular porosity ($n_0 = 0.3$–0.6).

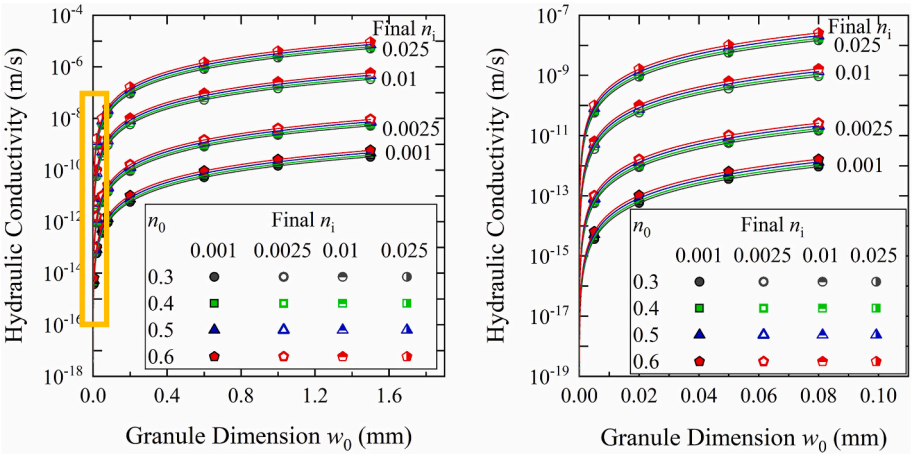

Fig. 10. Hydraulic conductivity vs. primary granule dimension (w_0) for different initial intergranular porosity (n_0) and final intergranular porosity (Final n_i): (a) entire range of predominant granule dimension (w_0) and (b) close up for w_0 between 0.00 and 0.08 mm (outlined with orange box in "a").

achieve low hydraulic conductivity.

Very low final intergranular porosity (n_i) is required to achieve hydraulic conductivities on the order of 10^{-11} m/s, typical of GCLs permeated with dilute solutions (e.g., Shackelford et al., 2000; Jo et al., 2001; Kolstad et al., 2004). For the smallest granules, n_i must be no more than 0.025, and for large granules n_i must be less than 0.001 (Fig. 10). The controlling factor in all cases is the width of the intergranular pore throats (w_t), as illustrated in Fig. 11. Hydraulic conductivities on the order of 10^{-11} m/s require $w_t < 0.16$ μm.

3.3. Comparison with observations in GCLs

These findings are consistent with experimental observations from hydraulic conductivity tests conducted on GCLs using solutions that have different effect on swelling of bentonite granules during hydration. When granular bentonites are permeated with solutions that constrain granule swell substantially (e.g., high ionic strength solutions), little granule swelling occurs, large intergranular pores persist during permeation, and the hydraulic conductivity is high (10^{-6} to 10^{-4} m/s, comparable to sand). The hydraulic conductivity of a GCL with powdered bentonite that is permeated with the same solution will be elevated, but not as high (10^{-9} to 10^{-6} m/s, comparable to a lean clay or silt (Petrov and Rowe 1997, Jo et al., 2001; Benson et al., 2010; Chen et al., 2018; Li et al., 2021; Norris et al., 2022a,b). In constrast, for permeant solutions that promote granule swelling during hydration (e.g., deionized water), the granules swell substantially and intergranular pores are nearly non-existent, resulting in very low hydraulic conductivity regardless of whether the unhydrated bentonite is granular or powdered (Jo et al., 2001; Kolstad et al., 2004; Benson et al., 2010; Li et al., 2021).

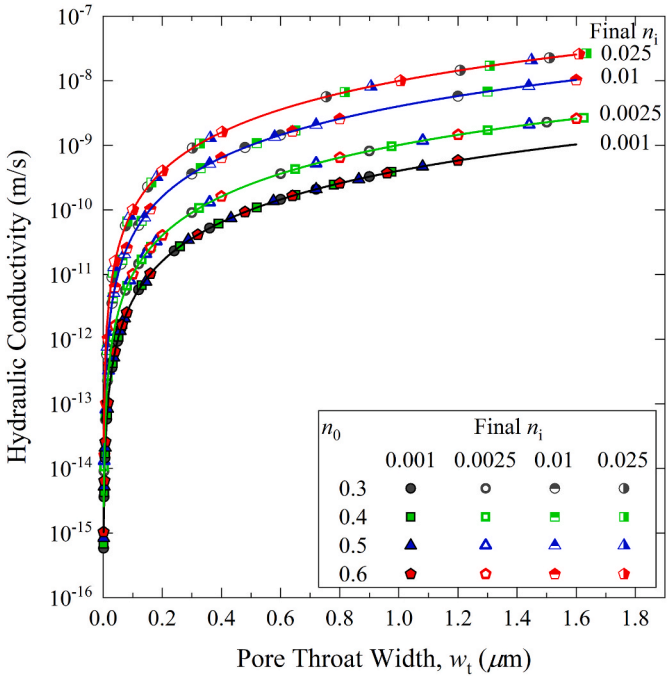

Fig. 11. Hydraulic conductivity of domain as a function of pore throat width (w_t) for different initial intergranular porosities (n_0) and final intergranular porosities (Final n_i).

4. Summary and practical implications

A hydrodynamic model was developed to provide quantitative evidence supporting the conceptual model that the hydraulic conductivity of bentonite in GCLs diminishes as the bentonite granules swell in response to hydration, decreasing the size of the intergranular pores conducting flow. The model does not address alterations in the bentonite that might occur if the permeant solution or physical condition changes subsequent to hydration and swelling.

The model simulates flow in an idealized GCL containing equi-sized and equi-spaced square bentonite granules stacked vertically in a rectangular grid and separated by intergranular pores. Water was assumed to flow only within the intergranular pores (i.e., the granules were assumed impermeable). Granule swelling was assumed to occur uniformly and homogeneously in the domain, with the increase in granule size occurring within adjacent intergranular pores. The hydrodynamic model was implemented within COMSOL Multiphysics 5.4, a multipurpose partial differential equation solver employing the finite element method. The model was parameterized with granule sizes and bentonite densities consistent with the conditions in GCLs.

Predictions made with the hydrodynamic model are consistent with the premise that the hydraulic conductivity of GCLs diminishes as the bentonite granules swell during hydration, with the hydraulic conductivity decreasing orders of magnitude as swelling granules fill intergranular pores through which the permeant solution flows. Greater swelling is required to achieve low hydraulic conductivity when GCLs contain larger granules or have lower bentonite density. For this reason, the hydraulic conductivity of GCLs with bentonite comprised of larger granules is more sensitive to chemical interactions that suppress osmotic swelling of the montmorillonite fraction of the bentonite. These

outcomes from the hydrodynamic model are consistent with experimental data reported for GCLs containing bentonites with different granule size.

These findings suggest that GCLs can be engineered to be more resilient and less sensitive to chemical interactions that influence swelling of the bentonite during hydration. In particular, GCLs containing bentonite with granules that have smaller intergranular pores (smaller granule size, higher bentonite density, more broadly graded granule sizes) are expected to have hydraulic conductivity that is less sensitive to interactions with hydrating and permeant solutions that suppress granule swelling.

Data availability

No data were used for the research described in the article.

APPENDIX

Acknowledgement

Financial support for Hou's contributions to this study was provided by the National Natural Science Foundation of China (NSFC) (Nos. 51978390, 51778353), 2023 Basic Research Program of Qinghai Province (2023-ZJ-756), and the China Scholarship Council (CSC 201906895014). Financial support for Benson's contributions to this study was provided by the US Department of Energy's Consortium for Risk Evaluation with Stakeholder Participation (CRESP) III through Cooperative Agreement No. DE-FC01-06EW07053.

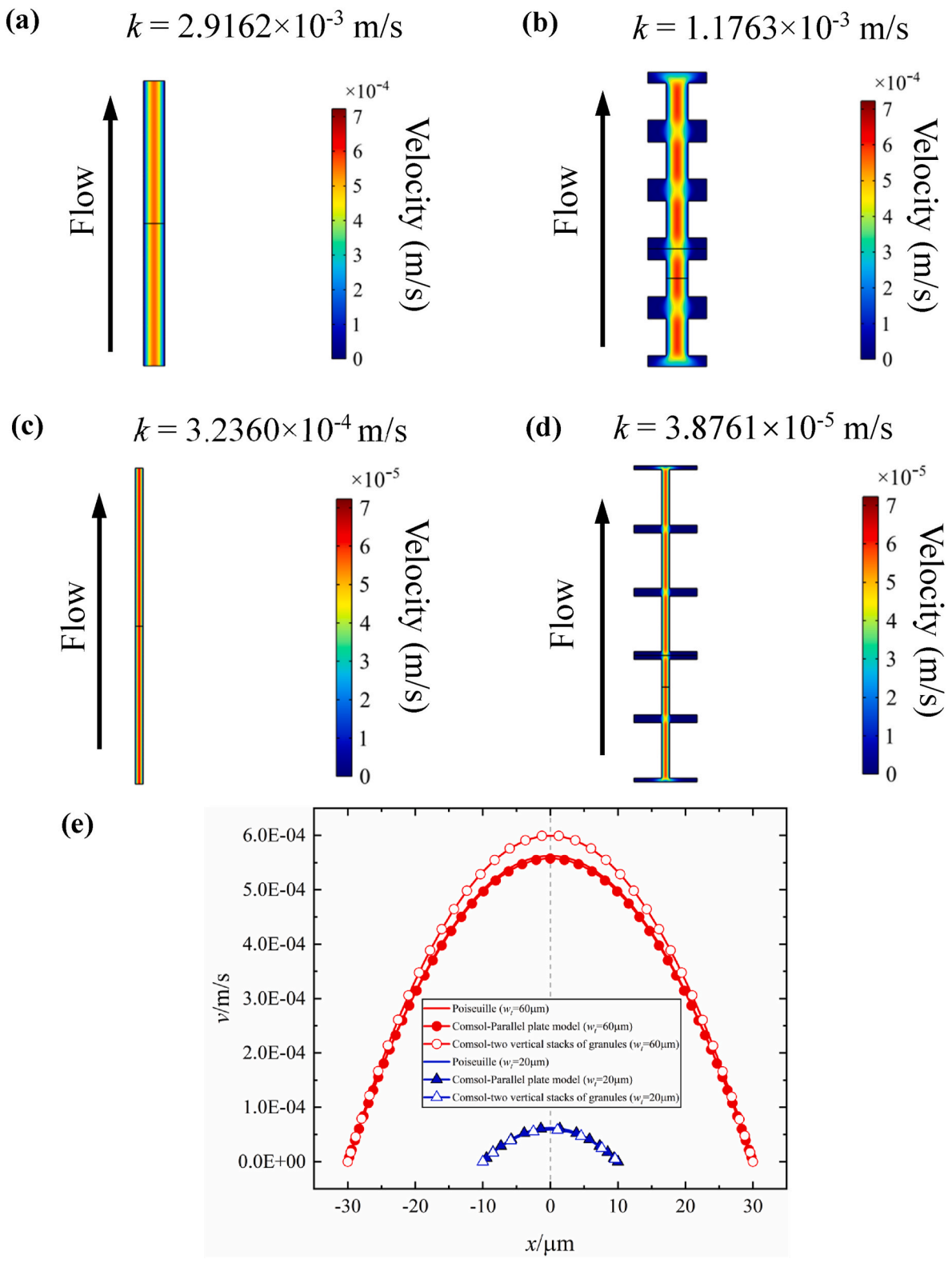

Fig. A1. Flow between parallel plates ($w_t = 60$ μm) (a), flow in the pore space between two vertical stacks of granules ($w_t = 60$ μm) (b), flow between parallel plates ($w_t = 20$ μm) (c), flow in the pore space between two vertical stacks of granules ($w_t = 20$ μm) (d), and comparison of velocity field predicted by COMSOL to the velocity field for flow between parallel plates as defined by the Hagen-Poiseuille equation described in Panton (2013).

References

Bareither, C.A., Zadeh, S.G., Conzelmann, J., Scalia, J., Shackelford, C.D., 2017. Evaluation of mechanical and hydraulic properties of geosynthetic clay liners for mining applications. Tail. Mine Waste 2017, 1–9, 2017.

Benson, C.H., Oren, A.H., Gates, W.P., 2010. Hydraulic conductivity of two geosynthetic clay liners permeated with a hyperalkaline solution. Geotext. Geomembr. 28 (2), 206–218.

Bradshaw, S.L., Benson, C.H., 2014. Effect of municipal solid waste leachate on hydraulic conductivity and exchange complex of geosynthetic clay liners. J. Geotech. Geoenviron. Eng. 140 (4), 1–17.

Chen, J.N., Benson, C.H., Edil, T.B., 2018. Hydraulic conductivity of geosynthetic clay liners with sodium bentonite to coal combustion product leachates. J. Geotech. Geoenviron. Eng. 144 (3), 1–12.

COMSOL, 2021. COMSOL Multiphysics® V. 5.4 Software Package. COMSOL AB, Stockholm.

Gustitus, S.A., Nguyen, D., Chen, J.N., Benson, C.H., 2021. Quantifying polymer loading in bentonite-polymer composites using loss on ignition and total carbon analyses. Geotech. Test J. 44 (5), 1448–1466.

Hou, J., Sun, R., Chu, C.X., Karen, M., Nasser, M., 2022. A numerical study of chemical compatibility of GCLs. Appl. Sci. 12 (4), 2182.

Jo, H.Y., Katsumi, T., Benson, C.H., Edil, T.B., 2001. Hydraulic conductivity and swelling of nonprehydrated GCLs permeated with single-species salt solutions. J. Geotech. Geoenviron. Eng. 127 (7), 557–567.

Kolstad, D.C., Benson, C.H., Edil, T.B., 2004. Hydraulic conductivity and swell of nonprehydrated geosynthetic clay liners permeated with multispecies inorganic solutions. J. Geotech. Geoenviron. Eng. 130 (12), 1236–1249.

Li, Q., Chen, J.N., Benson, C.H., Peng, D.P., 2021. Hydraulic conductivity of bentonite-polymer composite geosynthetic clay liners permeated with bauxite liquor. Geotext. Geomembr. 49 (2), 420–429.

Norris, A., Aghazamani, N., Scalia, J., Shackelford, C.D., 2022a. Hydraulic performance of geosynthetic clay liners comprising anionic polymer-enhanced bentonites. J. Geotech. Geoenviron. Eng. 148 (6), 1–16.

Norris, A., Scalia, J., Shackelford, C.D., 2022b. Mechanisms controlling the hydraulic conductivity of anionic polymer-enhanced GCLs. Geosynthetics Intl. online.

Panton, R., 2013. Incompressible Flow. John Wiley & Sons, Inc., New York.

Petrov, R.J., Rowe, R.K., 1997. Geosynthetic clay liner (GCL)-chemical compatibility by hydraulic conductivity testing and factors impacting its performance. Can. Geotech. J. 34 (6), 863–885.

Rowe, R.K., 2020. Geosynthetic clay liners: perceptions and misconceptions. Geotext. Geomembr. 48 (2), 137–156.

Scalia, J., Benson, C., Edil, T., Bohnhoff, G., Shackelford, C.D., 2011. Geosynthetic Clay Liners Containing Bentonite Polymer Nanocomposite, GeoFrontiers 2011 Advances in Geotechnical Engineering. GSP No. 211, ASCE, Reston, VA, pp. 2001–2009.

Scalia, J., Bohnhoff, G., Shackelford, C.D., Benson, C.H., Sample-Lord, K., Malusis, M., Likos, W., 2018. Enhanced bentonites for containment of inorganic waste leachates by GCLs. Geosynth. Int. 1072–6349, 1–20.

Shackelford, C.D., Benson, C.H., Katsumi, T., Edil, T.B., Lin, L., 2000. Evaluating the hydraulic conductivity of GCLs permeated with non-standard liquids. Geotext. Geomembranes.

Tian, K., Likos, W.J., Benson, C.H., 2019. Polymer elution and hydraulic conductivity of bentonite-polymer composite geosynthetic clay liners. J. Geotech. Geoenviron. Eng. 145 (10), 1–12.